

ANALYSIS OF TURBULENT FLOW WITHIN AN AXIAL TURBINE USING CFD AND ITS COMPARISON WITH 2D DESIGN TOOL BASED ON A SMALL GAS TURBINE ENGINE REQUIREMENTS

V. G. Monteiro, J. T. Tomita, C. Bringhenti, J. F. C. Monteiro
 Aeronautics Institute of Technology, ITA
 São José dos Campos, São Paulo, 12.228-900
 Gas Turbine Group
 Brazil

Abstract

The present work is a project developed between ITA, IAE/APA and TGM Aerospace. ITA is the Brazilian Aeronautical Institute of Technology (Engineering school), IAE is the Aeronautical and Space Institute and APA is the gas turbine division at IAE. All of them are institutes of DCTA (Science and Technology Aerospace Department). TGM Aerospace is a Brazilian steam turbine manufacturer and together with DCTA are owners of the intellectual property of the axial turbine evaluated in this study. The turbine design requirements were determined by thermodynamic cycle calculations for a small jet engine in thrust range of 5kN. The single-stage axial flow turbine was designed adopting an in-house code that uses the meanline technique considering forced vortex assumption with the addition of Kacker and Okappuu loss modeling to quantify the internal loss sources as tip leakage, secondary flow, shock wave formation, trailing edge effects and profile losses. The 3D geometry of this turbine was generated making the use of a CAD software. This geometry was used to perform the mesh generation process. The fillet regions at turbine hub and tip regions were considered to become the turbine geometry more realistic. A commercial CFD solver was used to calculate the governing equations based on Reynolds-Averaged Navier-Stokes with the addition of turbulence model. The two-equation Shear-Stress Transport (SST) turbulence model was used to account the effects of

flow eddy viscosity. The results show a good agreement of both numerical tools and the importance of a simple design technique to obtain the turbine preliminary sizing. Flow properties distribution along the blade span were compared and discussed.

Nomenclature

H_0	Total Enthalpy
H_0'	Isentropic Total Enthalpy
\dot{m}	Mass flow
$\dot{m}_{corrected}$	Corrected mass flow
MUSCL	Monotone Upstream-Centered Schemes for Conservation Laws
η_t	Total to total isentropic efficiency
P_0	Total pressure
T_0	Total temperature
t	Torque
n_{blades}	Number of rotor blades
ω	Angular velocity

Subscripts

in	Turbine inlet
out	Turbine outlet
blades	Rotor blades

Introduction

Several turbomachines design techniques were developed aiming enhancements in its design process since 1D meanline models until 3D turbulent flow calculations via CFD. Reduced order models equipped with appropriate loss correlations, supplies good results during the preliminary machine sizing design phase. Meanline techniques are capable to calculate the turbomachine

design-point and their performance in several operational conditions. Thus, its maps can be synthesized using 1D models and its results can be used as input data into 2D models as streamline curvature method.

Hardware developments push CFD techniques to a high level of numerical simulations, in which, it is possible to observe and evaluate more details of 3D turbulent flow calculations and its characteristics in some key regions as near wall surfaces, where boundary layers are found (1).

According to Denton (2), the design of a modern turbine has been unthinkable without the use of CFD techniques, due to the good performance prediction, based on the use of many numerical aspects such as accuracy and physical representation of the flow for both regimes, steady and unsteady. The accuracy of the CFD predictions for turbomachines at its design point operation conditions are around $\pm 2\%$ for efficiency (3). This level of prediction is adequate to eliminate poor aerodynamic flow characteristics. CFD techniques are vastly used to enhance engineering designs with direct impact in project costs, mainly due to the lower number of tests.

The use and applications of the techniques above described is clearly reported by Dorney (4). Dorney studied a two-stage supersonic flow turbine and demonstrated the turbine design and off-design performance calculation, including some unsteady operational condition based on the changes of flow conditions through the machine. The flow characteristics were better analyzed after the 3D calculations using Reynolds Averaged Navier-Stokes (RANS) equations. The solutions from both, meanline and CFD numerical tools were compared and good agreement was observed in the results over a wide range of operational conditions. The 3D solution was also used to take decision of different locations

and positions to install transducers along the turbine to perform bench tests.

In this work, a single-stage axial flow turbine was designed by DCTA/IAE/APA staff and TGM Aerospace industry. The turbine was designed based on the engine data requirements obtained during the development phase of thermodynamics cycle determination. A meanline code with forced vortex method, considering constant nozzle angle and constant momentum were used for the turbine design-point calculations to obtain the preliminary machine sizing (5). For off-design condition a meanline code, in which the internal losses were determined using the loss modeling developed by Denton (6), was used to calculate the turbine map. These data, also were used to generate the turbine 3D geometry making the use of SolidWorks®. This phase is essential to create an environment where the mesh will be generated to discretize the physical domain in numerical domain. The CFD simulations were performed, using the commercial software ANSYS® CFX v.15, at steady state regime. The appropriate boundary-conditions were obtained from meanline code and the formulation was based on RANS equations, with the addition of the two-equation turbulence model. Shear Stress Transport (SST) was set to account the flow eddy viscosity effects. The results of CFD solutions were synthesized to allow the analysis of flow characteristics distributions along the blade span at different streamwise locations.

Axial Turbine Geometry and Grid Generation

The turbine dimensions were firstly determined by the meanline code. After several adjustments of design parameters and its requirements, the geometry was constructed using SolidWorks® and then exported to the mesh generation process.

The CFD solution is highly dependent of the mesh quality. Depending on the control volumes distributions,

orthogonality, edge angles and smoothing, a good solution can be obtained due to the numerical issues as discretization errors and its order, mainly in regions close to the wall and discontinuities. For the 3D turbulent flowfield calculation, it is necessary to generate the mesh carefully in regions with boundary-layer. Hence, for each turbulence model, there are different requirements of y^+ to ensure good boundary-layer resolution.

In this work, due to the complexity of the turbine geometry, after the inclusion of a fillet at blade hub and tip (stator and rotor rows), the use of hexahedral elements penalized the mesh quality in the fillet regions. To improve the mesh refinements and control volumes quality in that region, an unstructured element type was used, based on tetrahedrons, due to their ability to match the elements and their faces in complex surfaces. The mesh was generated using the commercial software ICEM-CFD v.15, developed by ANSYS®.

The mesh generated after several tests and mesh configurations is shown in Figure 1 and Figure 2.

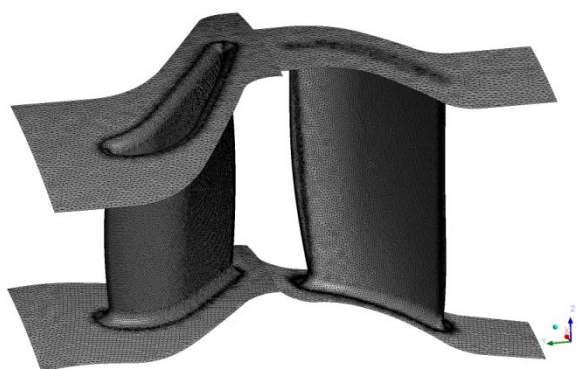


Figure 1 - Surface mesh details at stator and rotor rows.

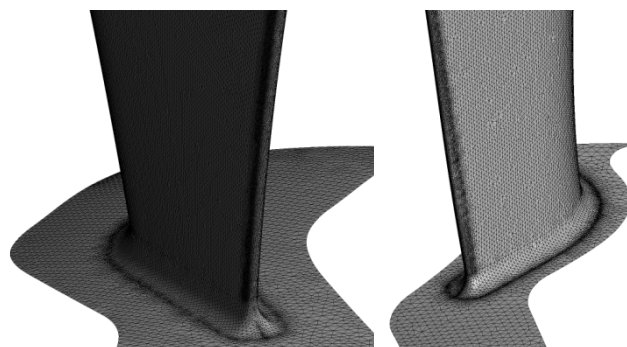


Figure 2 - Surface mesh with close-up at stator(left) and rotor (right) leading edges with fillet.

The use of unstructured mesh for the geometry with fillets regions is a good strategy to obtain a 3D discretized domain. Moreover, good control volumes quality were achieved at rotor tip clearance region.

Several attempts were made during the mesh generation process to achieve a good control volume distribution and to preserve the turbomachine geometrical details. The mesh has size of 706,832 elements in the stator domain and 1,150,083 in the rotor domain.

Boundary conditions

The work fluid adopted is the ideal gas with heat capacity at constant pressure varying with the temperature according to NASA Format (7).

The following boundary-conditions were imposed at surfaces:

- At inlet: total pressure and temperature; turbulence intensity and velocity vector angles.
- At walls: non-slip conditions.
- At outlet: static pressure at hub and distribution of static pressure along the blade span making the use of radial equilibrium equation.
- At blade-to-blade passages: rotational periodicity.
- At blade inter-rows: mixing-plane approach.

Table 1 shows the values adopted in the boundary conditions.

Table 1 - Boundary Condition

Total pressure at inlet (Pa)	476,228
Total Temperature at Inlet (K)	1,173
Rotational speed (rpm)	28,150
Static pressure at outlet (Pa)	170,752
Turbulence intensity	5%

Numerical Simulation Tools

Based on the data from thermodynamics cycle calculations of a small turbojet engine in the thrust class of 5kN, the axial turbine design requirements were obtained and its preliminary sizing started. An in-house numerical tool was used to determine the preliminary characteristics of the turbine: flow angles, blade dimensions, streamwise dimensions, diameters, internal flow and associated losses based on the models proposed by Denton (8). The turbine performance data is another module of this in-house code, in which the data from the design-point calculations are put into the performance module as input data to evaluate its operational conditions varying pressure ratio and rotational speed. All flow and fluid properties are recalculated at off-design conditions. In this work, the turbine performance was calculated for different mass-flow values at design-point rotational speed using the meanline technique.

Using the geometrical data obtained from meanline code, the 3D turbine geometry was generated by CAD software and to start the mesh generation process to discretize the physical domain in computational domain, where the fluid mechanics equations (continuity, momentum and energy) are calculated numerically for each control volume.

The CFD was conducted considering steady-state regime and Reynolds Averaged Navier-Stokes (RANS) equations, making the use of a commercial software CFX v.15®. The solver uses a pressure-

based and coupled algorithm, in which the pressure-velocity coupling is determined using the modified Rhie-Chow (9) discretization method for the convective terms, similar to the method proposed by Majumdar (10), (11).

For spatial integration of convective and diffusive terms an element-based finite volume method was used based on upwind scheme. In the CFX® software there is an option called high resolution schemes, that means an upwind with the addition of a MUSCL and limiter function to increase the order of discretization and to control this order inside of the computational domain. Hence, in regions where discontinuity effects are found, as shock wave formation, the scheme back to the original first order method and far from discontinuity regions the MUSCL and limiter function will increase the discretization order (two is the maximum order, but rarely this value is reached due to the mesh geometrical characteristics and flow behavior). The limiter function used by the solver follow the model proposed by Barth and Jespersen (12).

For time integration, an implicit time-step scheme was adopted based on the automatic time scale over the entire flow domain (for all control volumes) to allow the solver to perform the numerical procedure with high Courant number ensuring its good numerical stability.

For the diffusion terms were adopted a parametrical coordinates interpolation called shape functions (11). This methodology has been showed very robust and usual in finite elements method.

The two-equation Shear-Stress Transport (SST) turbulence model, developed by Menter (13), was used to account the flow eddy viscosity effects. The convective terms from turbulence equations are calculated using the high resolution scheme as aforementioned for the momentum equations.

There are no general rule to stop the numerical iterations. The expertise of the CFD staff will determine the most appropriate criteria. In this work, was monitored the residuals from the continuity and momentum equations, including the mass-flow variations at turbine inlet and outlet and its efficiency. The numerical stabilization of these variables can indicate if the solution is converged or not. These numerical behaviors during the iterations are presented in Figure 3, Figure 4 and Figure 5.

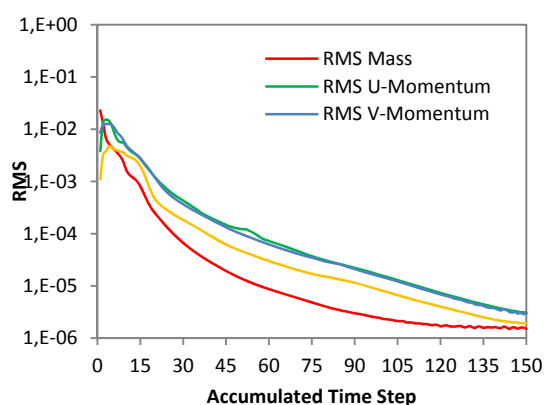


Figure 3 - Continuity and momentum equations residues decayment.

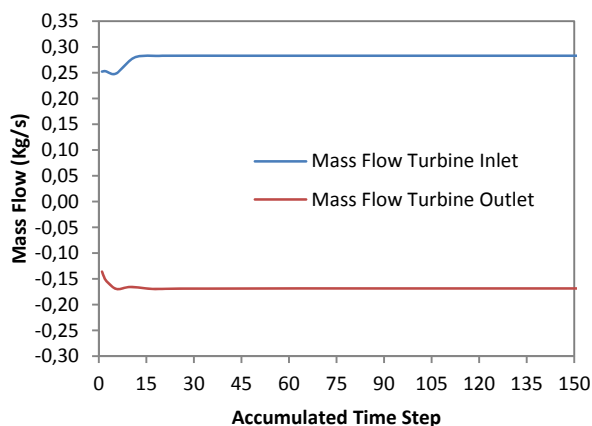


Figure 4 - Mass-flow variation and stabilization during the numerical procedure.

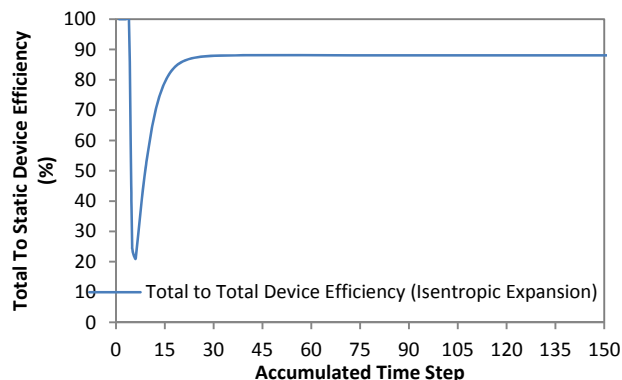


Figure 5 - Total to total isentropic efficiency variation and stabilization during the numerical procedure.

Comparison Between the Results from Different Numerical Tools

The CFD tool was used to verify the consistency of the results obtained making the use of meanline codes, during the preliminary design phase. The 3D flow calculations is more realistic and with its results it is possible to observe more details of the flow behavior along the turbine flow passage.

Table 2 shows the comparisons between the meanline code with forced vortex method (used in the turbine preliminary design-point calculations), meanline code with the addition of loss modeling based on reference (8), to determine the turbine off-design condition and the 3D CFD solver. All these results are related with design-point operation.

Table 2 - Comparison Between Meanline and 3D CFD Results

	Forced Vortex Method	3D CFD Simulation	Meanline + Denton Loss Modeling
Mass Flow (kg/s)	7.91	7.92	7.51
Power (W)	1.724E+06	1.719E+06	1.621E+06
Total to total isentropic efficiency	89.69%	88.08%	88.09%

The values presented in Table 2 are, in general, in a good agreement. Differences can be observed for the mass flow and power calculated by meanline code with Denton loss modeling, when compared with the forced vortex method and 3D CFD simulation. The difference in the turbine power is from mass-flow differences. Due to the simplicity of Denton loss model to calculate the boundary-layers effects (14), the meanline code can over estimating some internal loss aspect. One-dimensional loss models are not capable to estimate the boundary-layer characteristics with the same accuracy than CFD.

Figures 6 to 11 shows the comparison of Mach numbers, pressure and temperature distributions along the blade span for different turbine streamwise locations, at design-point, using the meanline forced vortex method and 3D CFD solver.

Note that, at blade hub and tip regions the differences are greater between the meanline and CFD results. This is due to the very simple technique and modeling used by meanline code to account the boundary-layer effects (velocity distribution close to the walls). The average values for each turbine streamwise location, within the range of 20% - 80% blade span, are in agreement for both design numerical tools.

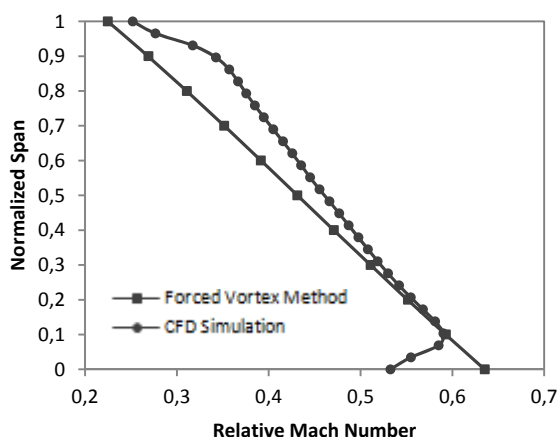


Figure 6 - Relative mach number at rotor inlet.

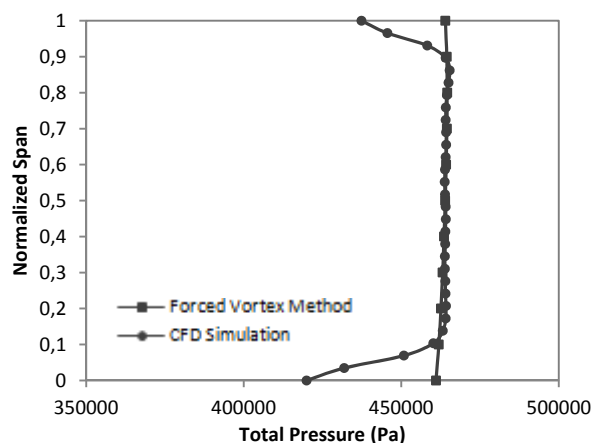


Figure 7 - Total pressure at rotor inlet.

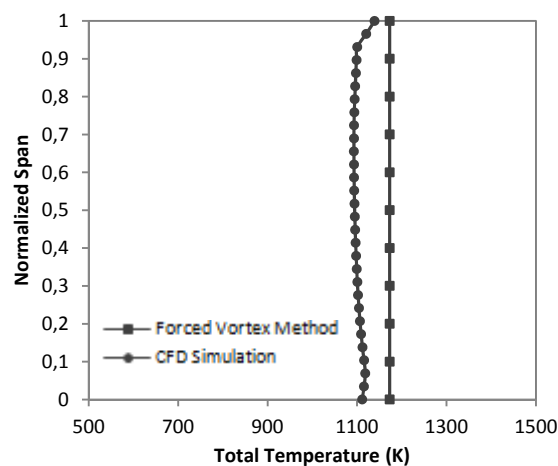


Figure 8 - Total temperature at rotor inlet.

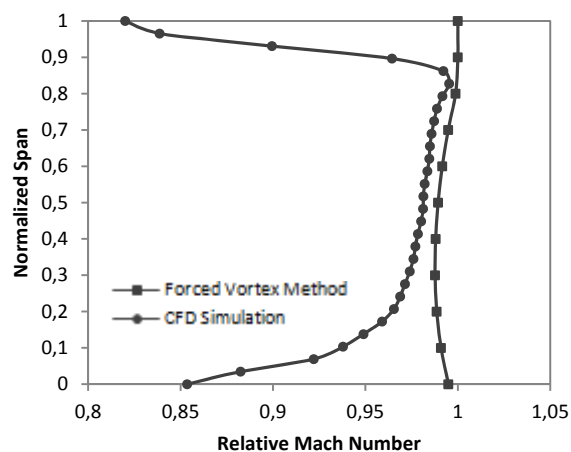


Figure 9 - Relative Mach Number at rotor outlet.

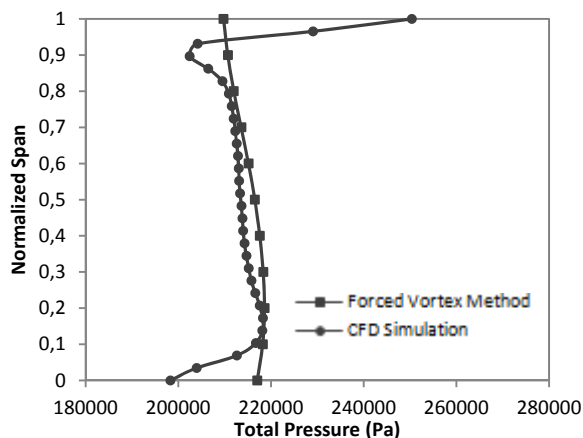


Figure 10 - Total pressure at rotor outlet.

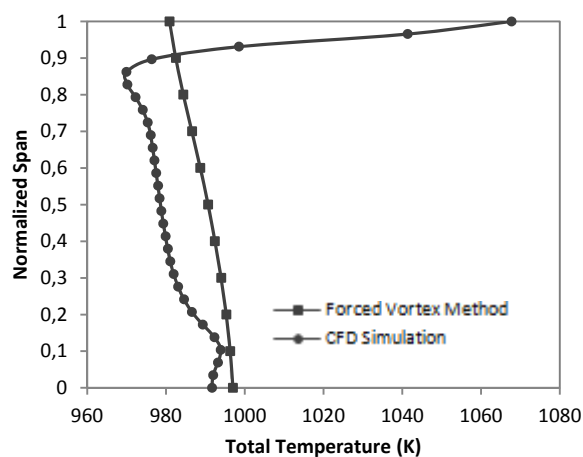


Figure 11 - Total temperature at rotor outlet.

Figure 12 shows the variation of the stage degree of reaction. An average difference of 10% was observed between the results from meanline and 3D CFD. The degree of reaction has influence on the blade angles and velocity triangles aspects. Based on the results from Figures 13 and 14, it is possible to observe that the main differences of absolute flow angles along the blade span are located at rotor row outlet. The dissipation of internal losses and its behavior due to the existence of different loss sources as secondary, tip, mixing, profile and shock wave losses are better represented in the 3D flow calculations. The 3D flow calculations from CFD solver is more accurate due to the inclusion of viscous effects in the momentum equations,

including the turbulence effects quantified by two-equation turbulence model.

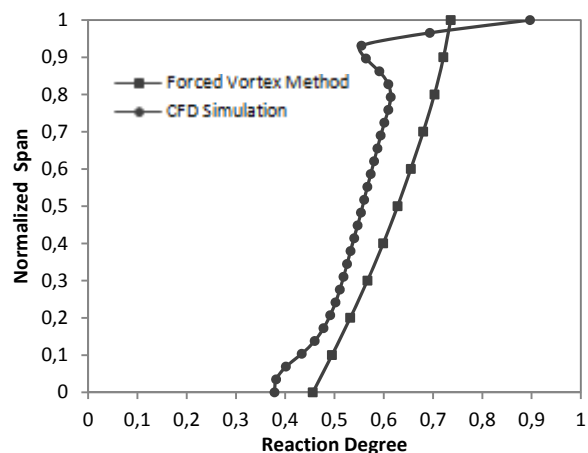


Figure 12 - Stage Reaction degree.

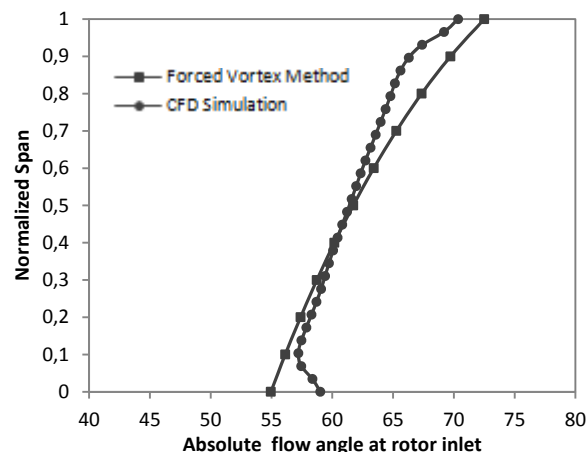


Figure 13 - Absolute angle distribution at rotor inlet.

Figures 15 and 16 show the distributions of the relative flow angles at rotor row inlet and outlet locations. In general, the relative flow angles values from both numerical tools are in agreement, not only qualitatively, but quantitatively too.

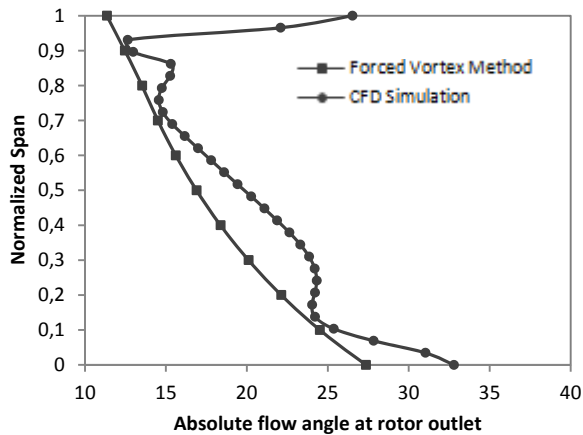


Figure 14 - Absolute angle distribution at rotor outlet.

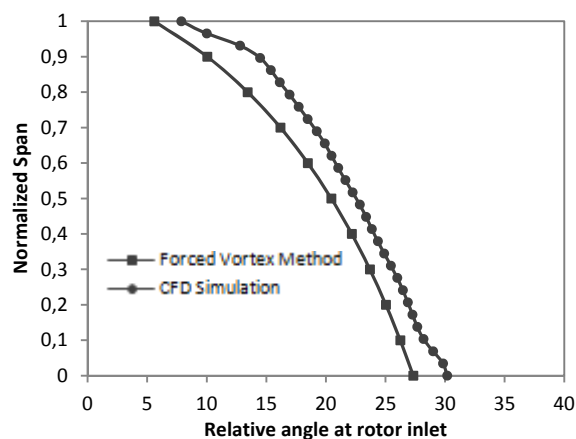


Figure 15 - Relative angle distribution at rotor inlet.

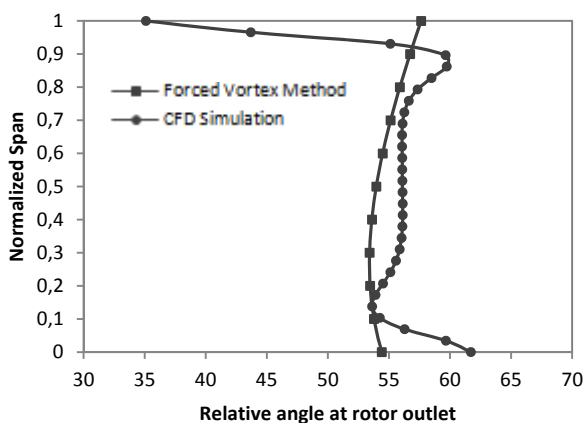


Figure 16 - Relative angle distribution at rotor outlet.

The results from CFD simulation shows with more details the variations of flow angles at rotor tip region, when

compared with the meanline technique for the curves at rotor outlet location.

Axial Turbine Performance Map at Design-Point Speed

The axial turbine performance map were synthesized using CFD software and meanline technique with loss modeling, developed by Denton (8) and implemented in the performance code (15) The off-design operational conditions were determined varying the static pressure at turbine outlet with constant rotational speed. The axial turbine performance curves are presented in Figs 17 and 18, in which the efficiency and pressure ratio variations for different corrected mass flow can be observed.

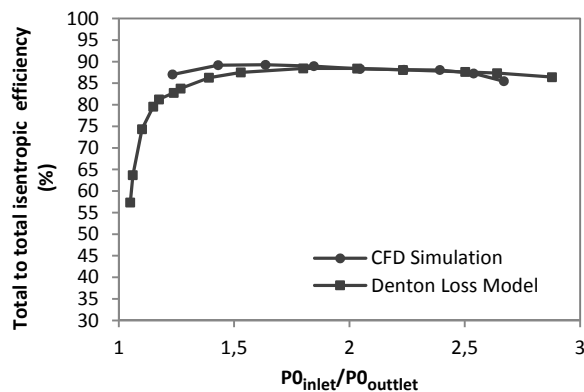


Figure 17 - Performance map of isentropic efficiency versus pressure ratio.

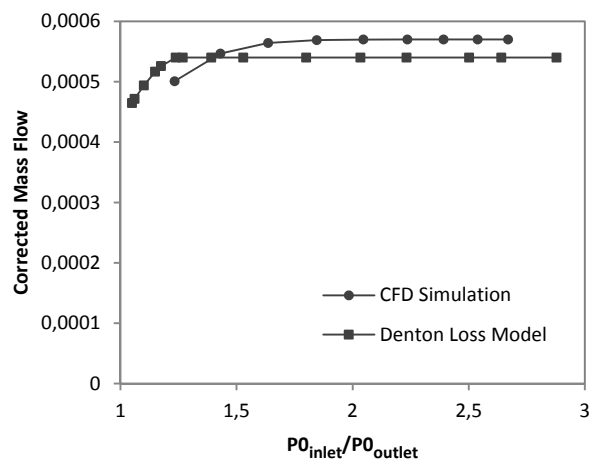


Figure 18 - Performance map of corrected mass flow versus pressure ratio.

The turbine power variation for different pressure ratio are presented in Fig. 19.

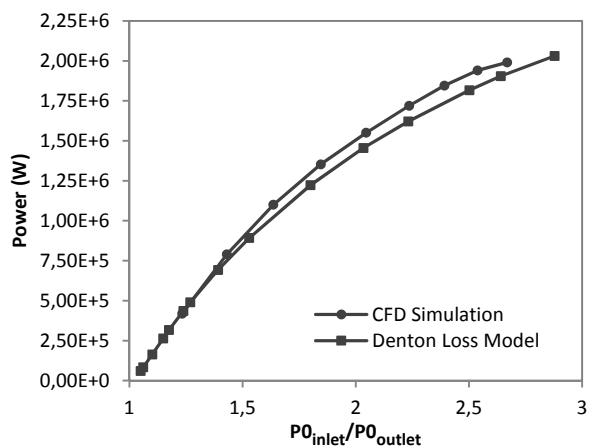


Figure 19 - Performance map of power versus pressure ratio.

In general, the results from both numerical tools are in good agreement, however, the pressure ratio that the turbine can be considered choked are quite different: In the meanline code the value is 1.2 and in the CFD solver the value is 1.8. As discussed earlier, the difference can be attributed to simplifications inherent of the loss model (simplification of the velocity distribution along the blades). Due to the fact that, the blade airfoil geometry, in the case of meanline analysis is not well defined, small variations in the blade-to-blade area and its velocity distributions at pressure and suction sides are not accurate when compared with 3D flow calculations. The turbine efficiency for both numerical tools are in good agreement.

3D Flowfield Calculation at Design-Point

Some flow characteristics were analyzed based on CFD results. Figures 20 and 21 shows the Mach number and static pressure contours for different blade span position: 10%, 50% and 90%.

With these results it is possible to observe that the stator row is operating under choking condition close to the hub region and the rotor row is operating under choking condition close to the tip region. These results are in agreement with the axial turbine literature. Figure 21 show the gas

expansion along the turbine streamwise direction.

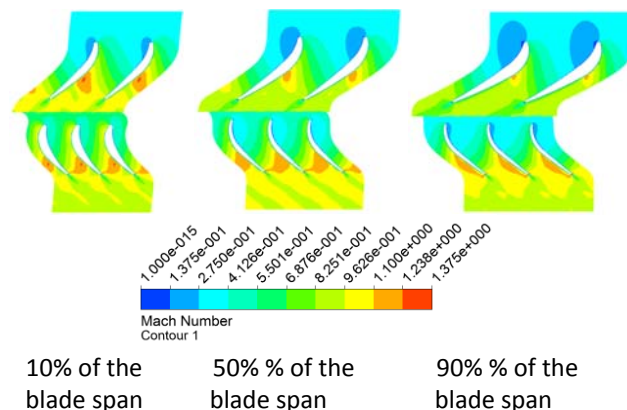


Figure 20 - Mach number contours at different blade span.

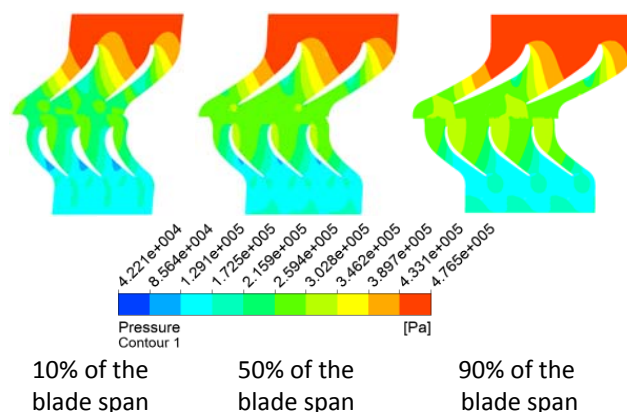


Figure 21 - Static pressure contours at different blade span.

Figure 22 show the streamline distribution along the turbine streamwise direction at 50% of blade span. There are no reserve flow on blade pressure and suction surfaces.

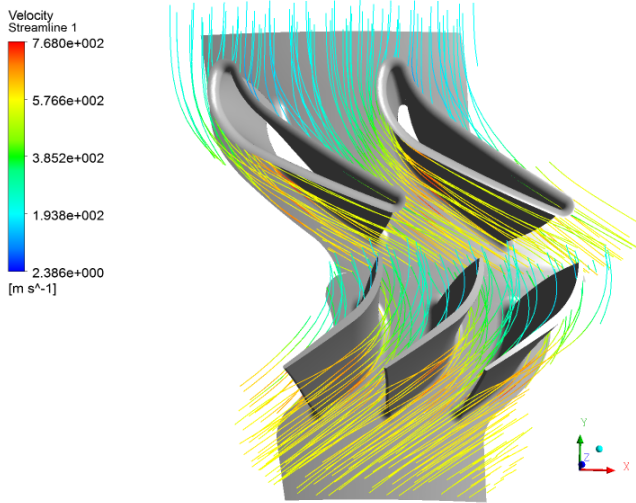


Figure 22 -Streamline along the turbine stage.

Figures 23 and 24 show the streamlines close to the rotor clearance region. Figure 25 presents the velocity vectors and the flow vertical structure in the rotor tip close to the blade leading edge.

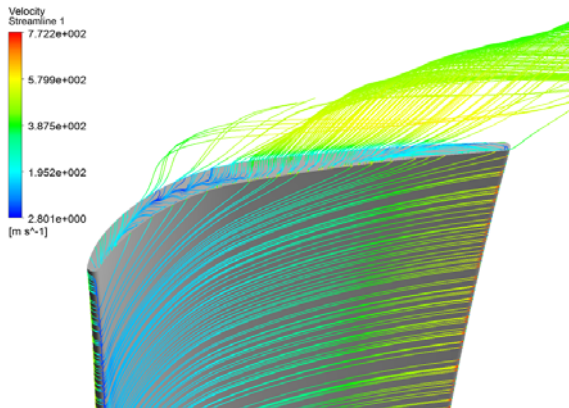


Figure 23 - Streamline at rotor tip - pressure side.

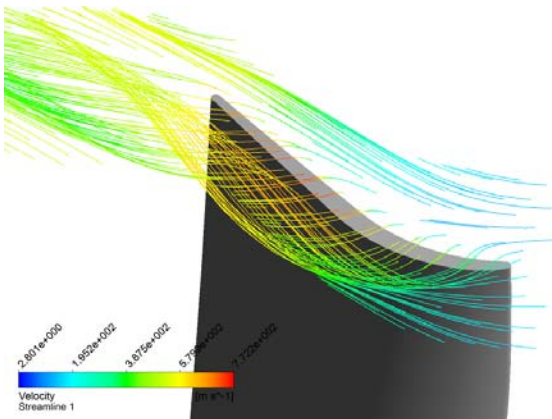


Figure 24 - Streamline at rotor tip - suction side.

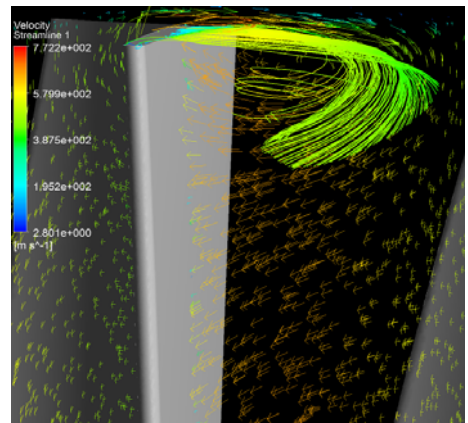


Figure 25 - Velocity vectors at rotor tip.

For turbines, the tip leakage usually is responsible by 1/3 of total losses. Figure 26 presents the static entropy contour at rotor tip. In this region, occurs the mixture process between the secondary and main flows that results in viscous dissipation and this energy will deteriorate the turbine power. Several researches study different rotor tip desensitization methods to improve the turbine performance decreasing the leakage effects.

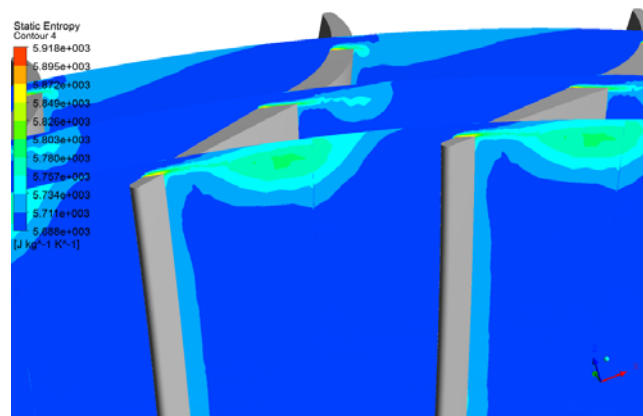


Figure 26 - Static Entropy at the tip leakage of the rotor suction side.

Conclusion

The results from different numerical tools used in the axial turbine design were compared. The well known reduced order meanline technique was used to perform the preliminary sizing

of an axial flow turbine following its design requirements determined from a small jet engine.

After several geometric and design parameter adjustments in the design code, the turbine geometry dimensions and its operational conditions was used as input data into the turbine performance code, in which the loss modeling developed by Denton (8) was implemented. The turbine 3D geometry was generated using CAD software, after that an unstructured mesh was generated to discretize the physical domain in computational domain, when the governing equations are calculated by CFD solver.

The performance map determined in this work, is in good agreement for both tools. As presented in Figure 17 the choking point are different comparing the 1D and CFD results. To decrease these differences the turbine blade airfoil can be adjusted to modify its throat area in the blade-to-blade plane.

In general, the results between these different numerical tools are in agreement. Some calibration and adjustments in the meanline performance code can be performed to improve the loss calculations mainly in terms of boundary-layer at turbine walls (blades and channel) including the existence of fillet region that is not accounted in the preliminary turbine sizing, but was consider in the 3D CFD calculation.

Annex

The total-to-total isentropic efficiency (η_t), corrected mass flow ($\dot{m}_{corrected}$) and power were calculated by the following equations, respectively:

$$\eta_t = \frac{H_{0\text{ in}} - H_{0\text{ out}}}{H_{0\text{ in}} - H'_{0\text{ out}}} \quad [1]$$

$$\dot{m}_{corrected} = \frac{\dot{m} \sqrt{T_{0\text{ in}}}}{P_{0\text{ in}}} \quad [2]$$

$$Power = \frac{t * n_{blades} * \omega}{1\text{ rad}} \quad [W] \quad [3]$$

Acknowledgements

The authors would like to thank the Turbomachines Departments at ITA, CNPq, CAPES, FAPESP, IAE/APA and TGM Aerospace for the support to this work.

Reference

1. **Casey, M.** Computational Methods for Preliminary Design and Geometry Definition in Turbomachinery. *Turbomachinery Design Using CFD - AGARD LECTURE SERIES 195*. 1994.
2. **Denton, J. D. and Dawes, W. N.** Computational Fluid Dynamics for Turbomachinery Design. *IMechE* . 1999, Vol. 213.
3. **Casey, M.** Best Praticice Advice for CFD in Turbomachinery Design . *QNET-CFD Network Newsletter, No.3*. 2003, Vol. 2.
4. **Dorney, D. J. and Griffin, L. W.** Off-Design Performance of a Multi-Stage Supersonic Turbine. *American Institute of Aeronautics and Astronautics*. 41 th Aerospace Sciences Meeting & Exhibit, 2003.
5. **Monteiro, J. F. C.** *Projeto do Estágio de Turbina Axial*. Brazil : Internal Technical Report of Institute of Aeronautics and Space, 2009.
6. **Denton, J. D.** Loss Mechanisms in Turbomachines. *iMechE*. 1987.
7. **ANSYS.** CFX-Solver Modeling Guide: release v.15. 2009.
8. **DENTON, J. D.** The 1993 IGTI scholar lecture: loss mechanims in turbomachines. *Journal of Turbomachinery*. Oct. 1993, Vols. v. 115, p. 621-626.
9. **RHIE, C. M. and CHOW, W. L.** Numerical study of the turbulent flow

past an airfoil with trailing edge separation. *AIAA*. Paper 82-0998, 1982.

10. **MAJUMDAR, S.** Role of underrelaxation in momentum interpolation for calculation of flow with nonstaggered grids. *Numerical Heat Transfer*. 1988, Vol. v.13, pp. pp. 125-132.

11. *CFX-Solver Theory Guide: release 15*. **Ansys**. 2009.

12. **Barth, T. J. and Jespersen, D. C.** The Design and Application of Upwind Schemes on Unstructured Meshes. *AIAA*. Paper 89-0366, 1989.

13. **Menter, R. F.** Zonal Two Equation k-w Turbulence Models for Aerodynamic Flows. *24th Fluid Dynamics Conference*. AIAA-93-2906, 1993.

14. **Denton, J. D.** Loss Mechanisms in Turbomachines. *Journal of Turbomachinery*. 1993, Vol. 115.

15. **HESS, R.** Estudo comparativo de método de análise de desempenho de turbinas axiais, Dissertação de Mestrado. Aeronautics Institute of Technology: s.n., 2006.